Pergamon

PII: S0277-5387(97)00229-5

Polyhedron Vol. 16, No. 24, pp. 4265–4272, 1997

0277-5387/97 $17.00+0.00

Tetra(μ_3-hydroxo)hexa(μ_2-carboxylato-O,O′)-bridged tetranuclear terbium(III) cubane complex

Xiao-Ming Chen,[a]* Yu-Luan Wu,[a] Ye-Xiang Tong,[a] Ziming Sun[b] and David N. Hendrickson[b]*

[a] Department of Chemistry, Zhongshan University, 135 Xingang Rd. W., Guangzhou 510275, P.R. China

[b] Department of Chemistry-0358, University of California at San Diego, La Jolla, CA 92093, U.S.A.

(Received 24 April 1997; accepted 23 May 1997)

Abstract—A novel tetranuclear terbium(III) complex $[Tb_4(OH)_4(pybet)_6(H_2O)_8][Tb_4(OH)_4(pybet)_6(H_2O)_7(NO_3)](ClO_4)_{14}\cdot 6H_2O$ has been synthesized and shown by X-ray crystallography to have a cubane-like $Tb_4(\mu_3\text{-}OH)_4(\mu_2\text{-carboxylato-O,O}')_6$ core. The ligand pybet is pyridinoacetate, $C_5H_5\overset{+}{N}\text{-}CH_2CO_2^-$. Magnetic susceptibility data were measured for this Tb_4 complex in the range of 2.0–320 K and in fields of 1.0 G to 50.0 kG. It is concluded that either there is very weak antiferromagnetic exchange interaction ($J = -0.015\ cm^{-1}$) or there is a small crystal-field splitting of the $^7F_6$ Tb^{III} ground state. © 1997 Elsevier Science Ltd

Keywords: Terbium(III); cubane compound; carboxylate; hydroxide; crystal structure; magnetic properties.

In the past two decades cubane-like tetranuclear complexes have attracted considerable interest in bioinorganic chemistry and in magnetochemistry, since cubane complexes containing μ_3-sulfido or μ_3-oxo-bridges model the active site of some metalloenzymes and exhibit interesting magnetic properties. A large number of μ_3-sulfido bridged cubane-like metal complexes [1] and a number of μ_3-oxo and μ_3-alkoxo (or phenoxo)-bridged metal complexes [2] have been synthesized and subjected to extensive studies. Tetra(μ_3-hydroxo)-bridged cubane-like metal complexes are rare; only four examples have been reported for chromium(III) and three for copper(II) complexes without additional bridging ligand [3,4]. There is one example of a gadolinium(III) complex with the cube bicapped by two μ_3-aqua ligands [5].

In our attempt to prepare polynuclear lanthanoid(III) complexes containing pyridine betaine (IUPAC name: pyridinioacetate, $C_5H_5\overset{+}{N}\text{-}CH_2CO_2^-$, abbreviated as pybet) [6], we obtained an unusual tetranuclear Tb^{III} complex with the composition $[Tb_4(OH)_4(pybet)_6(H_2O)_8]$ $[Tb_4(OH)_4(pybet)_6(H_2O)_7(NO_3)](ClO_4)_{14}\cdot 6H_2O$ (**1**). There has been recent interest in characterizing the magnitude of magnetic exchange interactions between Ln^{III} ions in polynuclear complexes [7]. For example, Panagiotopoulos *et al.* [8] reported the structure and magnetochemistry of the dinuclear acetate-bridged complexes $[Ln_2(O_2CCH_3)_6(phen)_2]$, where Ln is either Ce^{III} or Gd^{III}. The susceptibility data for these complexes were fit to give magnetic exchange parameters of $J = -0.75\ cm^{-1}$ for the Ce^{III} complex and $J = -0.053\ cm^{-1}$ for the Gd^{III} complex. These interactions are considerably weaker than the Cu···Cu interaction present in $[Cu_2(O_2CCH_3)_6(H_2O)_2]$ [9] where $J = -147\ cm^{-1}$. Ferromagnetic Cu^{II}–Gd^{III} exchange interactions have been reported [10] for complexes containing both ions.

EXPERIMENTAL

Compound preparation

Pyridinoacetate (pybet) was synthesized with a literature method [11]. Solvents and reagents were used as purchased. To an aqueous solution (3 cm^3) of $Tb(NO_3)_3$ was added pybet (0.173 g, 1 mmol) and an ethanolic solution (2 cm^3) of *o*-phenanthroline (0.2 g, 1 mmol), followed by addition of an aqueous solution

* Authors to whom correspondence should be addressed.

of $NaClO_4$ (3 mmol). The resulting solution was stirred at 60°C for 20 min, and then allowed to evaporate slowly in air. After about a week, a colorless crystalline sample of complex **1** was obtained in high yield (*ca* 50%). The C, H, and N microanalyses were carried out with a Perkin–Elmer 240Q analyzer. Found: C, 24.51; H, 2.91; N, 3.24; Calc. for $C_{84}H_{134}N_{13}Cl_{15}O_{116}Tb_8$ (**1**): C, 24.24; H, 2.71; N, 3.45%.

Instrumentation

Variable-temperature dc magnetic susceptibility data were collected for a polycrystalline sample of complex **1** on a Quantum Design MPMS5 SQUID susceptometer equipped with a 55 kG magnet and operating in the range of 1.8–400 K. Alternating current (ac) susceptibility measurements were made with a MPMS2 SQUID equipped with a 10 kG magnet. The ac field was oscillated at 1000 Hz with an amplitude of 1 G and with a zero dc field. Diamagnetic corrections were estimated using Pascal's constants [12] and were subtracted from the experimental molar susceptibility to obtain the paramagnetic molar susceptibilities.

X-ray crystallography

A selected single crystal of **1** was used to collect X-ray data at 292 K on an Enraf–Nonius CAD4 diffractometer (Mo-Kα, $\lambda = 0.71069$ Å). Determination of the crystal class, orientation matrix, and cell dimensions were performed according to the established procedures; the intensity data were collected using the ω–2θ scan (5.0 min^{-1}) mode [13]. Two standard reflections were monitored after every 200 data measurements, showing only small random variations (< 1.5%). Data processing was carried out with the NRCVAX program package [14]. Crystallographic data are summarized in Table 1.

Most of the non-hydrogen atoms in the crystal structure of **1** were located with the direct methods of the SHELXS-86 program package [15] and subsequent Fourier syntheses were used to derive the remaining non-hydrogen atoms. All the non-hydrogen atoms were refined anisotropically except the two-fold disordered oxygen atoms of the perchlorate anions, which were subjected to geometric restraints. Hydrogen atoms of water molecules have not been located from the difference maps; hydrogen atoms of the pybet ligands were generated (C–H = 0.96 Å), assigned isotropic thermal parameters, and ride on their parent carbon atoms. All the hydrogen atoms were held stationary and included in the final state of full-matrix least-squares refinement using the SHELXL-93 program package [16]. Analytical expressions for the neutral-atom scattering factors were employed, and anomalous dispersion corrections were incorporated [17]. Selected bond lengths and angles are given in Table 2.

Table 1. Crystallographic data

Formula	$C_{84}H_{134}Cl_{15}N_{13}O_{116}Tb_8$
M	4985.15
Crystal system	triclinic
Space group	$P\bar{1}$
a(Å)	14.354(3)
b(Å)	17.827(4)
c(Å)	18.087(4)
α(°)	92.50(3)
β(°)	108.71(3)
γ(°)	96.39(3)
Z	1
D_c (kg m^{-3})	1.907
Crystal size (mm)	0.30 × 0.40 × 0.26
μ(Mo-Kα) (cm^{-1})	35.6
λ(Mo-Kα)(Å)	0.71069
No. of collected data	15204
No. of unique data	15204
No. of observed data [$I > 2\sigma(I)$]	11064
No. of refined parameters (p)	1167
R	0.0694
R_w	0.1928
S	1.043

RESULTS AND DISCUSSION

X-ray structure

The crystal structure of **1** shows discrete cubane-like tetranuclear $[Tb_4(OH)_4(pybet)_6(H_2O)_8]^{8+}$ and $[Tb_4(OH)_4(pybet)_6(H_2O)_7(NO_3)]^{7+}$ cations, perchlorate and lattice water molecules. In each of the cations, four Tb^{III} ions and four OH^- ions are alternately arranged at the corners of a distorted cubane. Six pybet ligands bridge the faces of each cubane unit. In each cubane-like core the four metal atoms are bridged by four μ_3-hydroxo and six μ_2-carboxylato-O,O′ bridges. As shown in Fig. 1, each Tb^{III} ion in the cubane-like core is linked to the other three Tb^{III} [Tb···Tb = 3.754(1)–3.900(2) Å] through three μ_3-hydroxo and three μ_2-carboxylato-O,O′ bridges. All the Tb—O bond lengths fall in range of 2.310(3)–2.558(3) Å, while the Tb—O—Tb bond angles are in range of 102.90(9)–110.38(11)°. Each of the Tb(1), Tb(2) and Tb(4) ions is in a distorted square-antiprismatic arrangement, being coordinated by the three μ_3-hydroxo ligands and three oxygen atoms of the μ_2-carboxylato-O-O′ groups [Tb—O(carboxy) = 2.310(3)–2.476(3) Å], and completed by two terminal aqua ligands [Tb—O(aqua) = 2.369(4)–2.558(3) Å]. Although the Tb(3) ion is also eight-coordinate, as illustrated in Fig. 2, each pair of the O(1s) positions of two crystallographically inversely-related cubane cores are occupied by an aqua ligand and an oxygen atom of a monodentate nitrato ligand, respectively; both the aqua oxygen atom and the nitrato atoms have half site occupancies. The pair of inversely-related cubane cores in the solid are linked into a dimer through a moderately strong hydrogen bond between

Table 2. Selected bond lengths (Å) and angles (°)

Tb(1)···Tb(3)	3.7562(9)	Tb(1)···Tb(4)	3.7582(11)
Tb(1)···Tb(2)	3.8456(14)	Tb(2)···Tb(4)	3.7539(12)
Tb(2)···Tb(3)	3.8821(11)	Tb(3)···Tb(4)	3.900(2)
Tb(1)—O(12)	2.310(3)	Tb(1)—O(42)	2.322(3)
Tb(1)—O(1)	2.362(3)	Tb(1)—O(3)	2.382(3)
Tb(1)—O(1w)	2.396(3)	Tb(1)—O(52)	2.433(3)
Tb(1)—O(2)	2.447(2)	Tb(1)—O(2w)	2.447(3)
Tb(2)—O(3)	2.335(2)	Tb(2)—O(31)	2.355(3)
Tb(2)—O(11)	2.358(4)	Tb(2)—O(2)	2.373(3)
Tb(2)—O(4)	2.389(3)	Tb(2)—O(61)	2.421(3)
Tb(2)—O(3w)	2.447(4)	Tb(2)—O(4w)	2.455(4)
Tb(3)—O(1)	2.339(2)	Tb(3)—O(21)	2.345(3)
Tb(3)—O(2)	2.355(3)	Tb(3)—O(32)	2.357(3)
Tb(3)—O(4)	2.394(3)	Tb(3)—O(5w)	2.442(3)
Tb(3)—O(1S)	2.459(3)	Tb(3)—O(41)	2.476(3)
Tb(4)—O(22)	2.324(4)	Tb(4)—O(62)	2.331(3)
Tb(4)—O(51)	2.336(3)	Tb(4)—O(3)	2.358(3)
Tb(4)—O(4)	2.402(2)	Tb(4)—O(6w)	2.423(3)
Tb(4)—O(1)	2.428(3)	Tb(4)—O(7w)	2.558(3)

O(12)—Tb(1)—O(42)	95.70(13)	O(12)—Tb(1)—O(1)	143.46(9)
O(42)—Tb(1)—O(1)	82.28(11)	O(12)—Tb(1)—O(3)	87.42(12)
O(42)—Tb(1)—O(3)	140.30(10)	O(1)—Tb(1)—O(3)	72.54(10)
O(12)—Tb(1)—O(1w)	81.3(2)	O(42)—Tb(1)—O(1w)	70.32(12)
O(1)—Tb(1)—O(1w)	130.47(14)	O(3)—Tb(1)—O(1w)	148.65(11)
O(12)—Tb(1)—O(52)	141.82(10)	O(42)—Tb(1)—O(52)	103.21(11)
O(1)—Tb(1)—O(52)	72.72(9)	O(3)—Tb(1)—O(52)	98.08(10)
O(1w)—Tb(1)—O(52)	74.50(13)	O(12)—Tb(1)—O(2)	73.90(10)
O(42)—Tb(1)—O(2)	73.86(10)	O(1)—Tb(1)—O(2)	70.51(9)
O(3)—Tb(1)—O(2)	69.06(9)	O(1w)—Tb(1)—O(2)	133.64(10)
O(52)—Tb(1)—O(2)	143.17(10)	0(12)—Tb(1)—O(2w)	73.52(11)
O(42)—Tb(1)—O(2w)	142.86(12)	O(1)—Tb(1)—O(2w)	127.36(10)
O(3)—Tb(1)—O(2w)	75.84(10)	O(1w)—Tb(1)—O(2w)	72.92(12)
O(52)—Tb(1)—O(2w)	71.38(11)	O(2)—Tb(1)—O(2w)	132.49(10)
O(3)—Tb(2)—O(31)	146.53(11)	O(3)—Tb(2)—O(11)	88.84(11)
O(31)—Tb(2)—O(11)	107.92(11)	O(3)—Tb(2)—O(2)	71.12(9)
O(31)—Tb(2)—O(2)	84.55(10)	O(11)—Tb(2)—O(2)	76.56(11)
O(3)—Tb(2)—O(4)	71.32(9)	O(31)—Tb(2)—O(4)	78.52(10)
O(11)—Tb(2)—O(4)	143.37(10)	O(2)—Tb(2)—O(4)	68.06(10)
O(3)—Tb(2)—O(61)	99.67(10)	O(31)—Tb(2)—O(61)	86.24(11)
O(11)—Tb(2)—O(61)	139.60(12)	O(2)—Tb(2)—O(61)	143.55(11)
O(4)—Tb(2)—O(61)	75.56(11)	O(3)—Tb(2)—O(3w)	75.69(11)
O(31)—Tb(2)—O(3w)	136.73(12)	O(11)—Tb(2)—O(3w)	70.90(13)
O(2)—Tb(2)—O(3w)	133.38(11)	O(4)—Tb(2)—O(3w)	129.19(11)
O(61)—Tb(2)—O(3w)	73.16(13)	O(3)—Tb(2)—O(4w)	146.40(13)
O(31)—Tb(2)—O(4w)	67.05(14)	O(11)—Tb(2)—O(4w)	75.55(14)
O(2)—Tb(2)—O(4w)	130.93(11)	O(4)—Tb(2)—O(4w)	136.16(13)
O(61)—Tb(2)—O(4w)	75.91(13)	O(3w)—Tb(2)—O(4w)	71.14(13)
O(1)—Tb(3)—O(21)	84.44(10)	O(1)—Tb(3)—O(2)	72.53(9)
O(21)—Tb(3)—O(2)	142.23(10)	O(1)—Tb(3)—O(32)	144.88(11)
O(21)—Tb(3)—O(32)	104.92(11)	O(2)—Tb(3)—O(32)	80.50(10)
O(1)—Tb(3)—O(4)	69.38(9)	O(21)—Tb(3)—O(4)	75.82(11)
O(2)—Tb(3)—O(4)	68.27(9)	O(32)—Tb(3)—O(4)	80.07(10)
O(1)—Tb(3)—O(5w)	76.09(10)	O(21)—Tb(3)—O(5w)	73.71(11)
O(2)—Tb(3)—O(5w)	126.23(10)	O(32)—Tb(3)—O(5w)	138.97(11)
O(4)—Tb(3)—O(5w)	135.53(9)	O(1)—Tb(3)—O(1S)	146.17(10)
O(21)—Tb(3)—O(1S)	74.78(11)	O(2)—Tb(3)—O(1S)	138.04(10)
O(32)—Tb(3)—O(1S)	67.74(12)	O(4)—Tb(3)—O(1S)	128.18(10)
O(5w)—Tb(3)—O(1S)	72.64(11)	O(1)—Tb(3)—O(41)	102.15(9)
O(21)—Tb(3)—O(41)	141.44(11)	O(2)—Tb(3)—O(41)	74.10(10)
O(32)—Tb(3)—O(41)	91.35(11)	O(4)—Tb(3)—O(41)	142.27(10)
O(5w)—Tb(3)—O(41)	71.27(10)	O(1S)—Tb(3)—O(41)	79.80(11)
O(22)—Tb(4)—O(62)	99.49(13)	O(22)—Tb(4)—O(51)	106.07(12)

Continued overleaf

O(62)—Tb(4)—O(51)	138.94(11)	O(22)—Tb(4)—O(3)	145.09(9)
O(62)—Tb(4)—O(3)	87.98(12)	O(51)—Tb(4)—O(3)	88.93(11)
O(22)—Tb(4)—O(4)	78.46(10)	O(62)—Tb(4)—O(4)	74.67(10)
O(51)—Tb(4)—O(4)	141.32(10)	O(3)—Tb(4)—O(4)	70.70(9)
O(22)—Tb(4)—O(6w)	70.52(12)	O(62)—Tb(4)—O(6w)	80.62(12)
O(51)—Tb(4)—O(6w)	78.40(12)	O(3)—Tb(4)—O(6w)	144.31(11)
O(4)—Tb(4)—O(6w)	136.14(10)	O(22)—Tb(4)—O(1)	81.82(11)
O(62)—Tb(4)—O(1)	141.44(9)	O(51)—Tb(4)—O(1)	74.77(9)
O(3)—Tb(4)—O(1)	71.80(10)	O(4)—Tb(4)—O(1)	67.81(9)
O(6w)—Tb(4)—O(1)	133.92(11)	O(22)—Tb(4)—O(7w)	143.02(11)
O(62)—Tb(4)—O(7w)	68.97(11)	O(51)—Tb(4)—O(7w)	71.27(11)
O(3)—Tb(4)—O(7w)	71.41(11)	O(4)—Tb(4)—O(7w)	127.48(10)
O(6w)—Tb(4)—O(7w)	72.92(12)	O(1)—Tb(4)—O(7w)	129.57(10)
Tb(3)—O(1)—Tb(1)	106.05(10)	Tb(3)—O(1)—Tb(4)	109.79(10)
Tb(1)—O(1)—Tb(4)	103.37(11)	Tb(3)—O(2)—Tb(2)	110.38(11)
Tb(3)—O(2)—Tb(1)	102.90(9)	Tb(2)—O(2)—Tb(1)	105.82(9)
Tb(2)—O(3)—Tb(4)	106.24(11)	Tb(2)—O(3)—Tb(1)	109.22(10)
Tb(4)—O(3)—Tb(1)	104.90(11)	Tb(2)—O(4)—Tb(3)	108.52(10)
Tb(2)—O(4)—Tb(4)	103.17(10)	Tb(3)—O(4)—Tb(4)	108.82(10)
N(1n)—O(1S)—Tb(3)	139.1(3)	C(11)—O(11)—Tb(2)	132.8(3)
C(11)—O(12)—Tb(1)	137.7(3)	C(21)—O(21)—Tb(3)	136.0(3)
C(21)—O(22)—Tb(4)	136.8(3)	C(31)—O(31)—Tb(2)	134.9(3)
C(31)—O(32)—Tb(3)	138.5(3)	C(41)—O(41)—Tb(3)	120.2(2)
C(41)—O(42)—Tb(1)	142.6(3)	C(51)—O(51)—Tb(4)	139.6(3)
C(51)—O(52)—Tb(1)	128.4(3)	C(61)—O(61)—Tb(2)	126.4(3)
C(61)—O(62)—Tb(4)	142.1(3)	O(11)—C(11)—O(12)	128.4(5)
O(22)—C(21)—O(21)	128.4(4)	O(32)—C(31)—O(31)	126.9(4)
O(41)—C(41)—O(42)	125.3(4)	O(51)—C(51)—O(52)	125.9(4)
O(62)—C(61)—O(62)	125.9(4)		

Hydrogen bonding

O(1w)···O(8w)	2.718(5)	O(4w)···O(9w)	2.640(10)
O(5w)···O(1n)	2.685(8)	O(1S)···O(2na)	2.756(9)
Tb(3)—O(1S)···O(2na)	129.3(2)	Tb(1)—O(1w)···O(8w)	141.9(2)
Tb(2)—O(4w)···O(9w)	90.1(2)	Tb(3)—O(5w)···O(1n)	97.6(2)
N(1n)—O(1n)···O(5w)	102.9(6)		

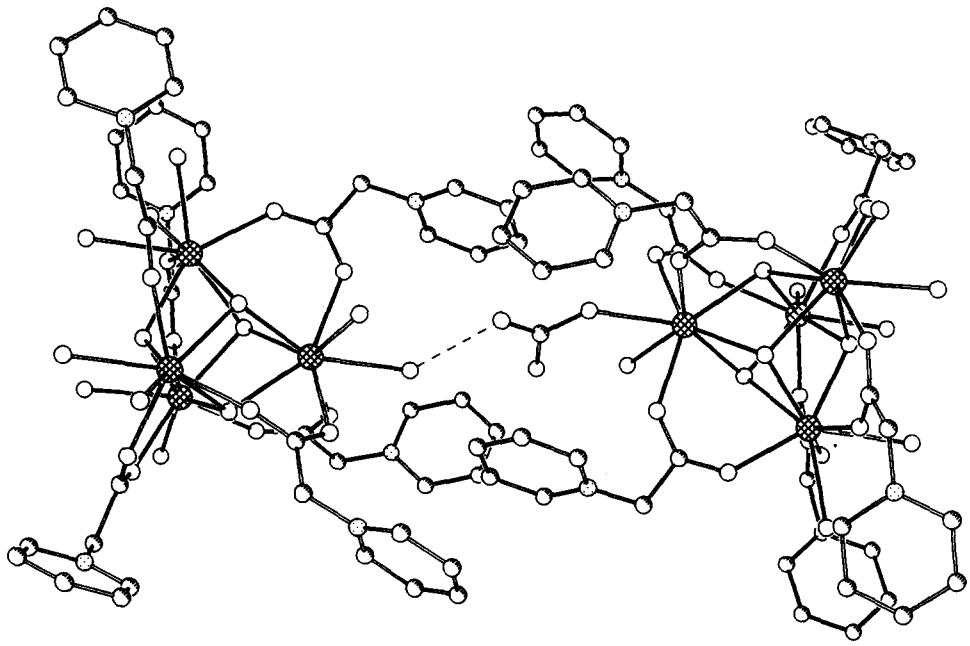

Fig. 1. Perspective view of complex **1** showing the hydrogen-bonded dimer of two inversely-related cubane-like cations. The hydrogen bond [O(1sa)···O(2n) = 2.78 Å] is represented by a broken line.

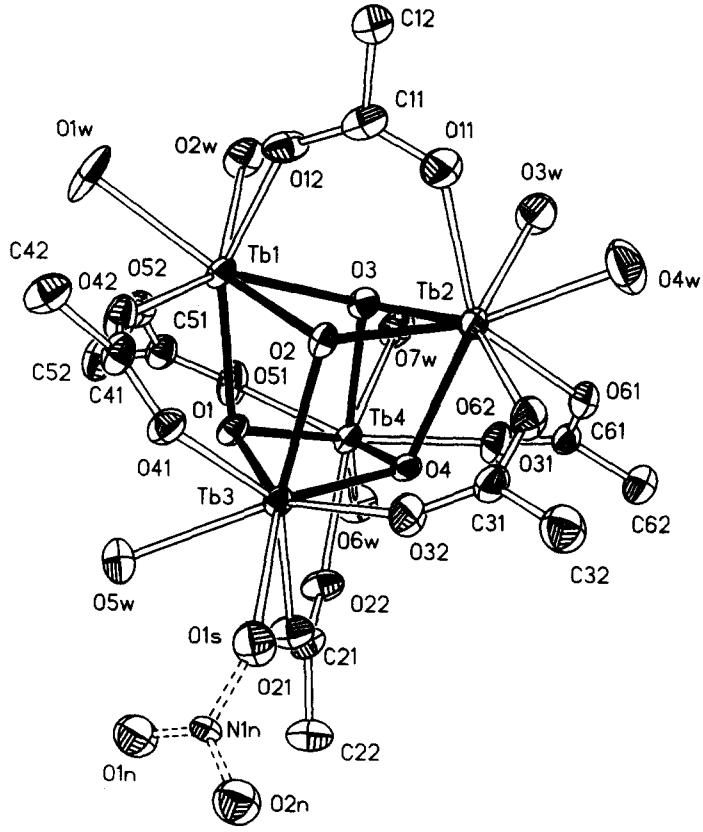

Fig. 2. ORTEP drawing (at 35% probability level) of the cubane-like core of complex **1**. The pyridinium groups are omitted for clarity. The site occupancies of the N(1n), O(1n) and O(2n) atoms are 0.5.

one of the uncoordinated nitrato oxygen atoms O(2n) and the aqua O(2s) atom [(O1s)···O(2na) = 2.756(9) Å].

Noteworthy is the fact that in contrast to the very extensively investigated μ_3-sulfido-, μ_3-oxo and μ_3-alkoxo (or phenoxo)-bridged cubane-line homo- and heterometallic complexes, there are only a few reported examples of μ_3-hydroxo-bridged cubane-like transition metal complexes [3,4], and only one example of cubane-like lanthanoid(III) complex, in which the cube is bicapped by two μ_2-aqua ligands [5]. Thus, the mixed (μ_3-hydroxo)(μ_2-carboxylato-O,O′)-bridged structure in complex **1** is unique.

Magnetochemistry

Since there has been very recently considerable interest [7,8] in the nature of magnetic exchange interactions between lanthanide ions in polynuclear complexes, the magnetochemistry of complex **1** was investigated. DC magnetic susceptibility data were collected for a polycrystalline sample of complex **1** in an external field of 10.0 kG. As can be seen in Fig. 3, the effective magnetic moment per molecule (μ_{eff}/molecule) is relatively constant in the 320–50 K range. varying from 18.83 μ_B at 319.9 K to 18.61 μ_B at 50.0 K. At lower temperatures μ_{eff}/molecule falls off to 11.2 μ_B at 2.01 K.

In contrast to transition metal ions, spin-orbit coupling in lanthanide ions is very strong. For such rare earth ions the interelectronic repulsions (e_2/r_{ij}) in the

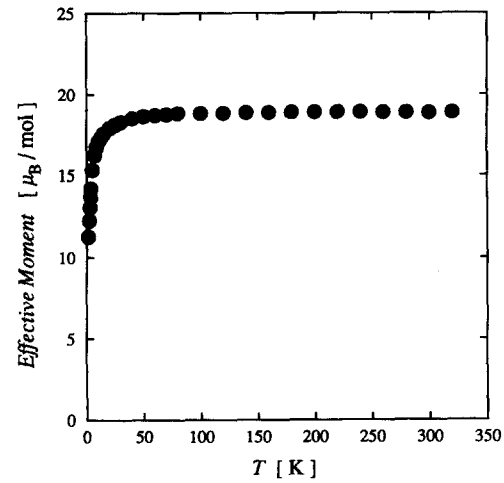

Fig. 3. Plot of the effective magnetic moment per molecule versus temperature for a polycrystalline sample of complex **1**. Data were collected in a 10.0 kG field.

f-manifold are larger than spin-orbit interactions and these are larger than the magnitude of crystal field effects. The 4*f* electrons are effectively shielded from their environment by the filled 5*s* and 5*p* subshells and, thus, the crystal-field interactions for the 4*f* electrons are quite small. The effect of the strong spin-orbit interaction is that the coupling between $\hat{L}$ and $\hat{S}$ is not broken by the crystal field and J is a good quantum number. The ground state of a Tb^{3+} ion is $^7F_6$ with a g factor of 3/2.

The van Vleck equation for the magnetic susceptibility of a $^7F_6$ Tb^{3+} ion gives $\mu_{eff} = 9.72\ \mu_B$. Thus, if there are no magnetic exchange interactions between Tb^{3+} ions in the tetranuclear Tb^{3+} complex **1**, the μ_{eff}/Tb_4 would be expected to be $\sqrt{4(9.72)^2}\ \mu_B = 19.4\ \mu_B$. This is close to the value of μ_{eff}/molecule of 18.83 μ_B measured for complex **1** at 320 K. Furthermore, from the relatively temperature independent nature (Fig. 3) of μ_{eff}/molecule observed for complex **1** in the 320–50 K range, it can be concluded that, if there are magnetic exchange interactions between the four Tb^{3+} ions in complex **1**, these interactions are quite weak. In reference to Fig. 3, the question then becomes whether the decrease in μ_{eff}/molecule seen below ~20 K for a sample of **1** in a 10.0 kG field is due to weak magnetic exchange interactions.

Since the $^7F_6$ ground state of a Tb^{3+} ion is of such a high multiplicity, it was important first to examine the magnetic field dependence of μ_{eff}/molecule at low temperatures. DC magnetic susceptibility data were collected in the low temperature region at several fields from 50.0 kG down to 500 G. In addition, ac susceptibility data were measured from 300 to 1.79 K in zero dc field, employing an ac field of 1.0 G oscillating at 1000 Hz. No out-of-phase ac signal was observed throughout the full temperature range. In Fig. 4 is given a plot of μ_{eff}/molecule measured below 30 K for complex **1** in the range of 50.0 kG to zero dc field. It is clear that the extent of decrease in μ_{eff}/molecule is dependent upon the magnitude of the external field. The larger the field is, the larger is the decrease in μ_{eff}/molecule. This is simply understood, for the $^7F_6$ Tb^{3+} ground state is split up into $(2J+1) = 13$ levels in a magnetic field. At the lowest temperatures the Boltzmann population of these 13 Zeeman levels is not equal if there is a relatively large (compared to kT at 2 K) Zeeman interaction due to a magnetic field.

Thus, an analysis of whether or not there are magnetic exchange interactions between the Tb^{3+} ions in complex **1** has to focus on the susceptibility data collected in zero dc field. These data are shown in Fig. 5, where it can be seen that in zero dc and 1.0 G ac field μ_{eff}/molecule only decreases to 13.7 μ_B at 1.79 K. The simplest possible spin Hamiltonian for the magnetic exchange interactions in complex **1** has only one exchange parameter 'Q'. We assume that the two different Tb_4 cubane cations are similar in their magnetic exchange interactions. Every possible $Tb^{3+} \cdots Tb^{3+}$ interaction in complex **1** was assumed

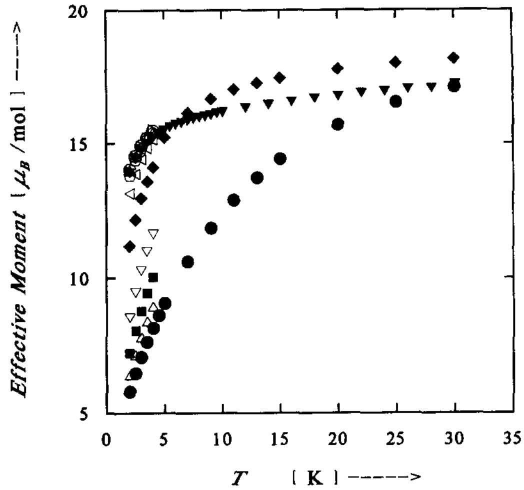

Fig. 4. Plot of the effective magnetic moment per molecule versus temperature for a polycrystalline sample of complex **1**. Data were measured in the 2.0–4.0 K range for the following magnetic fields: (△) 40.0 kG; (■) 30.0 kG; (▽) 20.0 kG; (●) 50.0 kG; (○) 2.0 kG; (▼) 1.0 kG; (○) 500 G. Data are also given in the 2.0–30.0 K range for the following magnetic fields: (●) 50.0 kG; (◆) 10.0 kG; and (▼) 1.0 G.

to be characterized by this parameter as given in the spin Hamiltonian in eqn (1):

$$\hat{H} = -2Q(\hat{J}_1 \cdot \hat{J}_2 + \hat{J}_1 \cdot \hat{J}_3 + \hat{J}_1 \cdot \hat{J}_4 + \hat{J}_2 \cdot \hat{J}_3 + \hat{J}_2 \cdot \hat{J}_4 + \hat{J}_3 \cdot \hat{J}_4) \quad (1)$$

The above equation is obviously based on the fact that J (= 6) is a good quantum number for each Tb^{3+} ion. By vector coupling the four Tb^{3+} ions spin

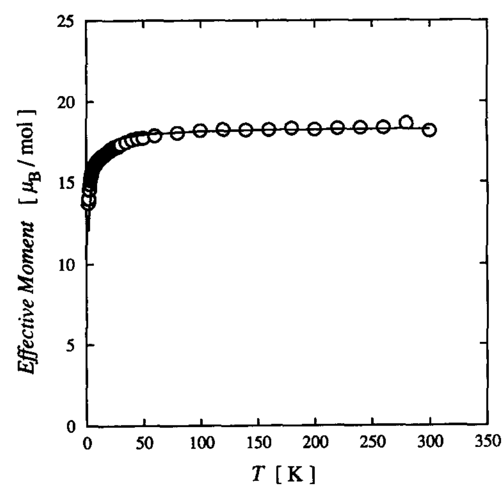

Fig. 5. Plot of the effective magnetic moment per molecule versus temperature for a polycrystalline sample of complex **1**. Data were measured in zero dc field with a 1.0 G ac field oscillating at 1000 Hz. The solid line represents the best fit of the data to the theoretical susceptibility expression derived from eqs (1) and (2).

together as $\hat{J}_T = \hat{J}_1 + \hat{J}_2 + \hat{J}_3 + \hat{J}_4$ it is possible to find an expression for the energies of the spin states of complex **1** as given in eq. (2).

$$E(J_T) = -Q[J_T(J_T+1)] \quad (2)$$

There are 1469 different spin states involving J_T values in the range $J_T = 24, 23, \cdots 1, 0$. Substitution of these energies and their corresponding degeneracies into the van Vleck equation gives a theoretical expression for the molar susceptibility of complex **1**, assuming there is only one exchange parameter Q.

The data shown in Fig. 5 (zero dc field) were least-squares fit to give $g = 1.41$ and $Q = -0.015$ cm^{-1} with the TIP value held constant at 600×10^{-6} cgsu. As can be seen in Fig. 5, the solid line representing this fit does accommodate the data reasonably well.

It is possible to improve the above fit by recognizing that the Tb_4 cubane units in complex **1** are not perfectly tetrahedral. In this case there would be two or perhaps three different exchange parameters Q. However, we did not elect to carry out fits with these different spin Hamiltonians, because there are other electronic interactions that may well account for the decrease in μ_{eff}/molecule at low temperatures in zero field. As has been discussed in detail by Gerloch and Mackey [18] the $^7F_6$ ground state of a Tb^{3+} ion in a complex can experience weak crystal field interactions that split the $^7F_6$ state. They studied the magnetochemistry of [Tb(antip)$_6$I$_3$], where antip is antipyrine (2,3-dimethyl-1-phenyl-Δ^3-pyrazolin-5-one). From a careful analysis of the temperature dependencies of the susceptibility for a single crystal of this antip complex they concluded that the crystal field splits the $^7F_6$ state into several states. Furthermore, at the lowest energies there are two states (A_{1g} and A_{2g} in the D_{3d} point group) that are separated by a very small energy. In effect, the splitting of the $^7F_6$ state by a weak crystal field gives a 'zero-field splitting'.

There are eight crystallographically different Tb^{3+} ions in complex **1**. Each has a similar eight coordination. The weak crystal field provided by the eight ligand atoms about each Tb^{3+} ion causes a splitting of the $^7F_6$ state. Since the site symmetry at each Tb^{3+} ion in complex **1** is quite low, the $^7F_6$ state for each Tb^{3+} ion could be split into several states. This gives a 'zero-field splitting' that could account for all of the decrease in μ_{eff}/molecule seen at low temperatures. It would be an enormous task to try to evaluate the effects of a crystal field splitting of the $^7F_6$ states for the Tb^{3+} ions in complex **1**. At the minimum one would need variable-temperature magnetic susceptibility data for a single crystal of complex **1**.

We have to conclude either that there is a very weak $Tb^{3+} \cdots Tb^{3+}$ magnetic exchange interaction of -0.015 cm^{-1} in complex **1** or, more likely, the decrease in μ_{eff}/molecule seen at low temperatures is due to crystal field splitting of the $^7F_6$ Tb^{3+} free-ion states. In the latter case the exchange coupling between Tb^{3+} ions could be negligible.

Acknowledgements—This work was supported by the National Science Foundation grant CHE-9420322 (D.N.H.) and by the NSFC and Natural Science Foundation of Guangdong (X.-M.C.).

REFERENCES

1. For recent examples see: (a) Yang, Y., Liu, Q.-T., Huang, L.-R., Kang, B.-S. and Lu, J.-X., *J. Chem. Soc., Chem. Commun.*, 1992, 1512; (b) Zhu, N.-Y., Zheng, Y.-F. and Wu, X.-T., *J. Chem. Soc., Chem. Commun.*, 1990, 780; (c) Chu, C. T.-W., Dahl, L. F. and Gall, R. S., *J. Am. Chem. Soc.*, 1982, **104,** 737; (d) Edelbult, A. W., Folting, K., Huffman, J. C. and Wentworth, R. A. D., *J. Am. Chem. Soc.*, 1981, **103,** 1927; (e) Lu, S.-F., Zhu, N.-Y., Wu, X-T., Wu, Q.-J. and Lu, J.-X., *J. Mol. Struct.*, 1989, **197,** 15; (f) Demadis, K. D., Chen, S.-J. and Coucouvanis, D., *Polyhedron*, 1994, **13,** 3147; (g) Liu, Q.-T., Yang, Y., Huang, L.-R., Wu, D.-X., Kang, B.-S., Chen, C.-N., Deng, Y.-H. and Lu, J.-X., *Inorg. Chem.*, 1995, **34,** 1884.
2. (a) McKee, V. and Shepard, W. B., *J. Chem. Soc., Chem. Commun.*, 1985, 158; (b) Bizilj, K., Hardin, S. G., Hoskins, B. F., Oliver, P. J., Tiekink, E. R. T. and Winter, G., *Aust. J. Chem.*, 1986, **39,** 1035; (c) Vreugdenhil, K., Haasnoot, J. G., Reedijk, J. and Spek, A. L., *Inorg. Chim. Acta*, 1987, **129,** 205; (d) Shi, S., Ji, W., Tang, S. H., Lang, J. P. and Xin, X. Q., *J. Am. Chem. Soc.*, 1994, **116,** 3615; (e) Shoner, S. C. and Power, P. P., *Inorg. Chem.*, 1992, **31,** 1001; (f) Kessissoglou, D. P., Raptopoulou, C. P., Bakalbassis, E. G., Terzis, A. and Mrozinski, J., *Inorg. Chem.*, 1992, **31,** 4339; (g) Hendrickson, D. N., Christou, G., Schmitt, E. A., Libby, E., Bashkin, J. S., Wang, S., Tsai, H.-L., Vincent, J. B., Boyd, P. D. W., Huffman, J. C., Folting, K., Li, Q. and Streib, W. E., *J. Am. Chem. Soc.*, 1992, **114,** 2455; (h) Wemple, M. W., Tsai, H.-L., Folting, K., Hendrickson, D. N. and Christou, G., *Inorg. Chem.*, 1993, **32,** 2025.
3. Akhter, L., Clegg, W., Garner, C. D. and Collison, D., *Inorg. Chem.*, 1985, **24,** 1725.
4. (a) Dedert, P. L., Ibers, J. A., Marks, T. J. and Sorrell, T., *Inorg. Chem.*, 1982, **21,** 3506; (b) Sletten, J., Sorensen, A., Julve, M. and Journaux, Y., *Inorg. Chem.*, 1990, **29,** 5054; (c) Real, J. A., Demunno, G., Chiappetta, R., Julve, M., Lloret, F., Journaux, Y., Colin, J. C. and Blondin, G., *Angew. Chem. Int. Ed. Engl.*, 1994, **33,** 1184.
5. Plakatouras, J. C., Baxter, I., Hursthouse, M. B., Malik, K. M. A., McAleese, J. and Drake, S. R., *J. Chem. Soc., Chem. Commun.*, 1994, 2455.
6. (a) Chen, X.-M., Wu, Y.-L. and Yang, Y.-S., *Aust. J. Chem.*, 1995, **48,** 1643; (b) Wu, Y.-L., Yang, Y.-S. and Chen, X.-M., *Acta Nat. Sci. Sunyatseni Univ.*, 1996, **35,** 66; (c) Yu, X.-L., Tong, M.-L. and Chen, X.-M., *Acta Nat. Sci. Sunyatseni Univ.*, 1996, **35,** 133; (d) Tong, M.-L., Zhou, Z.-Y., Wu, Y.-L. and Chen, X.-M., *Mal. J. Sci.*, 1996, **17B,** in press.
7. (a) Sakamoto, M., Hashimura, M., Matsuki, K.,

Tajima, K., Ishizu, K. and Okawa, H., *Bull. Chem. Soc. Jpn.*, 1991, **64,** 2835; (b) Li, X.-Y., Jiang, Z.-H., Liao, D.-Z., Yan, S.-P., Li, Y.-T. and Wang, G.-L., *Polyhedron*, 1994, **13,** 99; (c) Chen, X.-M., Aubin, S. M. J., Wu, Y.-L., Yang, Y.-S., Mak, T. C. W. and Hendrickson, D. N., *J. Am. Chem. Soc.*, 1995, **117,** 9600; (d) Liu, Z.-M., Liao, D.-Z., Jiang, Z.-H., Cheng, P., Liu, Y.-D. and Wang, G.-L., *Synth. React. Inorg. Met.-Org. Chem.*, 1995, **25,** 1249; (e) Deng, C.-L., Jiang, Z.-H., Liao, D.-Z., Yan, S.-P. and Wang, G.-L., *Synth. React. Inorg. Met.-Org. Chem.*, 1993, **23,** 247.

8. Panagiotopoulos, A., Zafiropoulos, T. F., Perlepes, S. P., Bakalbassis, E., Masson-Ramade, I., Kahn, O., Terzis, A. and Raptopoulou, C. P., *Inorg. Chem.*, 1995, **34,** 4918.
9. Güdel, H. U., Stebler, A. and Furrer, A., *Inorg. Chem.*, 1979, **18,** 1021.
10. (a) Benelli, C., Caneschi, A., Gatteschi, D., Guillou, O. and Pardi, L., *Inorg. Chem.*, 1990, **29,** 1750; (b) Bencini, A., Benelli, C., Caneschi, A., Dei, A. and Gatteschi, D., *Inorg. Chem.*, 1986, **25,** 572; (c) Sakamoto, M., Hashimura, M., Matsuki, K., Matsumoto, N., Inoue, K. and Okawa, H., *Bull. Chem. Soc, Jpn.*, 1991, **64,** 3639.
11. Chen, X.-M., Mak, T. C. W., *J. Chem. Soc., Dalton Trans.*, 1991, 3253.
12. Boudreaux, E. A. and Mulay, L. N., (eds), *Theory and Applications of Molecular Paramagnetism*, Wiley, New York (1976).
13. Frenz, B. A., *The Enraf–Nonius CAD4 SDP–A Real-Time System for Concurrent X-ray Data Collection and Crystal Structure Determination Package*, Enraf–Nonius, Deft, Holland (1978).
14. Gabe, E. J., Le Page, Y., Charland, J.-P. and Lee, F. C., *J. Appl. Cryst.*, 1989, **22,** 384.
15. Sheldrick, G. M., *SHELXS*-86, Program for X-ray Crystal Structure Refinement, University of Göttingen, Germany (1986).
16. Sheldrick, G. M., *SHELXL*-93, Program for X-ray Crystal Structure Refinement, University of Göttingen, Germany (1993).
17. *International Tables for X-ray Crystallography*, Vol. C, Tables 4.2.6.8 and 6.1.1.4; Kluwer: Dordrecht (1992).
18. Gerloch, M. and Mackey, D. J., *J. Chem. Soc. (A)*, 1971, 2605.